

Thermoanalytical study of precursors for In_2S_3 thin films deposited by spray pyrolysis

K. Otto · I. Oja Acik · K. Tõnsuaadu ·
A. Mere · M. Krunks

ESTAC2010 Conference Special Issue
© Akadémiai Kiadó, Budapest, Hungary 2011

Abstract Thermal decomposition of precursors for In_2S_3 thin films obtained by drying aqueous solutions of InCl_3 and $\text{SC}(\text{NH}_2)_2$ at the In:S molar ratios of 1:3 (**1**) and 1:6 (**2**) was monitored by simultaneous TG/DTA/EGA-FTIR measurements in the dynamic 80%Ar + 20%O₂ atmosphere. XRD and FTIR were used to identify the dried precursors and products of the thermal decomposition. The precursors **1** and **2** are complex compounds, while in **2** free $\text{SC}(\text{NH}_2)_2$ is also present. The thermal degradation of **1** and **2** in the temperature range of 30–900 °C consists of four mass loss steps, the total mass loss being 89.1 and 78.5%, respectively. According to XRD, In_2S_3 is formed below 300 °C, crystalline $\text{In}_{2.24}(\text{NCN})_3$ is detected only in **1** above 520 °C and In_2O_3 is the final decomposition product at 900 °C. The gaseous species evolved include CS_2 , NH_3 , $\text{H}_2\text{N}\text{CN}$, HNCS , which upon oxidation yield also COS , SO_2 , HCN and CO_2 .

Keywords TG/DTA · EGA-FTIR · Indium sulphide · Thiourea · Indium complex · Chemical spray pyrolysis · Ex situ FTIR and XRD

Introduction

Indium sulphide (In_2S_3) thin films are often used as buffer layers instead of CdS in chalcopyrite absorber layer based solar cells [1, 2]. Recently it was suggested that a transition

metal substituted In_2S_3 could be a promising absorber material for a new type of thin film solar cell exploiting two-photon processes [3]. In_2S_3 thin films can be manufactured by different physical and chemical deposition methods. Chemical spray pyrolysis (CSP) has been often used because it is an economical, rapid, non-vacuum and simple method to prepare thin films. In the CSP process, aqueous or alcoholic solutions containing InCl_3 and $\text{SC}(\text{NH}_2)_2$ (tu) as starting chemicals are pulverized in the form of fine droplets to the preheated substrate where In_2S_3 film is formed. CSP has been used to deposit In_2S_3 thin films with device quality properties, e.g., a buffer layer for solar cells [4, 5]. According to the literature, the main parameters influencing the properties of In_2S_3 thin films are the molar ratio of In and S sources (In:S) in the spray solution and the deposition temperature [5–7]. For example, the deposition of a sulphur-rich precursor solution with the In:S molar ratio of 1:6 minimizes oxide formation in the sprayed thin film [7]. However, the formation of In_2S_3 in the CSP process has not been studied in detail. Formation of In_2S_3 in the spray process is described by one reaction only: $2\text{InCl}_3 + 3\text{CS}(\text{NH}_2)_2 + 6\text{H}_2\text{O} \rightarrow \text{In}_2\text{S}_3 + 3\text{CO}_2 + 6\text{NH}_4\text{Cl}$ [8]. This general reaction seems to be too simple in the light of the studies performed on the formation of other metal sulphides, such as CdS, ZnS, SnS and Cu_xS in the CSP process. It is known that several complexes with different stoichiometry and water content are formed in aqueous solutions containing metal halogenides and thiourea [9–14], which upon their thermal decomposition lead to the formation of metal sulphides. Moreover, the molar ratio of the precursors in the spray solution may have a strong effect on the phase composition of the CSP-deposited metal sulphide films. For example, ZnS films prepared by spray of aqueous solutions containing ZnCl_2 and thiourea in the molar ratio of 1:1 comprise a ZnO impurity phase already at low growth temperatures in addition to the main phase of ZnS

K. Otto · I. Oja Acik · A. Mere · M. Krunks (✉)
Department of Materials Science, Tallinn University
of Technology, Tallinn, Estonia
e-mail: malle@staff.ttu.ee

K. Tõnsuaadu
Laboratory of Inorganic Materials, Tallinn University
of Technology, Tallinn, Estonia

[15]. Deposition of the solution with the Zn:S molar ratio of 1:2, which corresponds to the stoichiometry of dichlorobis(thiourea-*S*)-zinc(II) ($[\text{Zn}(\text{tu}_2)\text{Cl}_2]$), results in ZnS films with no ZnO phase at similar deposition temperatures [15].

Thermal decomposition of these metal halide thiourea complexes has been found to be a complicated multistep process [9–12, 16]. Generally, these complexes decompose at temperatures above 200 °C, leading to the formation of metal sulphides irrespective of the atmosphere. Metal sulphides are the final decomposition products in an inert atmosphere, however, in oxidative atmospheres metal oxides are the final products.

In(III) halides (InX_3) are known to form numerous five-coordinate and six-coordinate compounds with InX_3L_2 and InX_3L_3 -type molecules (L represents a ligand) [17]. It is also known that neutral sulphur-based donors, such as thioether and thiourea, form adducts with indium ion [17]. The crystal structure is known for $\text{InCl}_3\{\text{SC}(\text{NMe}_2)_2\}_2$ [18]. A probable interaction of the precursors in the spray solution is neglected [8].

The aim of this study was to obtain a better understanding of the formation of In_2S_3 films in the spray pyrolysis process. In order to follow the spray process, we prepared aqueous solutions containing InCl_3 and $\text{SC}(\text{NH}_2)_2$ in the molar ratio of 1:3 and 1:6, let the solvent evaporate, and characterized the dried samples in terms of their structure and elemental composition. Thermal decomposition of dried samples was monitored by simultaneous TG/DTA and EGA-FTIR methods in Ar + O₂.

Experimental

Chemicals and synthesis of samples

$\text{SC}(\text{NH}_2)_2$ (tu) (p.a. > 98%, Merck-Schnchardt S32896) and InCl_3 prepared from indium (p.a. 99.99%, Alfa Aesar) and concentrated HCl (Merck) were employed for the synthesis. All the chemicals were used as received without any further purification.

The precursor solutions were prepared by mixing 0.1 M InCl_3 and 0.75 M $\text{SC}(\text{NH}_2)_2$ aqueous solutions in the molar ratios ($\text{InCl}_3:\text{SC}(\text{NH}_2)_2$) of 1:3 (**1**) and 1:6 (**2**) at room temperature. In both cases, $[\text{In}^{3+}]$ was set to 5×10^{-2} mol/L. The solutions were let to slowly evaporate at 50 °C in a furnace for a week.

Characterization of dried precursors and products of their thermal decomposition

Fourier transformed infrared (FTIR) spectroscopy and X-ray diffraction (XRD) were used to characterize the dried powders **1** and **2** and the products of their thermal

decomposition. FTIR transmission spectra were measured in the region of 4000–400 cm^{−1} on a Perkin-Elmer GX1 spectrophotometer using the KBr pellet technique. XRD patterns were recorded by a Rigaku Ultima IV diffractometer with Cu K α radiation ($\lambda = 1.5406 \text{ \AA}$, 40 kV at 40 mA) using the silicon strip detector D/teX Ultra. The elemental composition of the dried samples **1** and **2** was determined by an Elemental Analysesysteme GmbH Vario EL CHNOS Elemental Analyser for S, C, N, H. Chlorine content was determined in **1** by the amperometric titration. In addition, heat treatments of **1** and **2** were performed in a preparative scale in air using a Nabertherm furnace. Heat treatment temperatures were determined on the basis of the dynamic TG runs.

Thermal analysis

TG/DTA measurements, coupled with the evolved gas analysis by FTIR (EGA-FTIR), were carried out on a SetSys-Evolution instrument connected to a Nicolet 380 FTIR spectrometer. The analyses were carried out in a dynamic 80%Ar + 20%O₂ (artificial air) atmosphere in the temperature range of 30–1000 °C using the heating rate of 10 °C min^{−1}, the gas flow rate of 60 mL/min and open Al_2O_3 crucibles. The initial mass of sample **1** was 7.8 mg and that of **2** was 7.4 mg. The gases evolved were led through a heated tube into a FTIR gas cell. The FTIR gas cell and the connecting tube were kept at 220 °C. The absorption spectra were recorded in the region of 4000–400 cm^{−1} with a resolution of 4 cm^{−1} and 60 scans averaged.

The evolved gases were identified on the basis of their FTIR reference spectra available in the literature [19] and in the public domain spectral libraries of NIST [20].

Results and discussion

Characterization of dried samples **1** and **2**

IR spectra of the dried samples **1** and **2** and that of free thiourea (tu) are compared in Fig. 1. The vibrations that peaked at 1473 and 1085 cm^{−1} in the spectrum of thiourea are characteristic of CN group stretching vibrations, $\nu(\text{CN})$ [9]. However, in **1** and **2**, the $\nu(\text{CN})$ vibrations are shifted to higher frequencies of 1504 and 1102 cm^{−1}, respectively. The increased wavenumbers of the CN group vibrations in **1** and **2** indicate the strengthening of the bond between carbon and nitrogen atoms [9, 21, 22]. IR spectrum of the free tu ligand exhibits strong and sharp vibrations at 1414, 730 and 630 cm^{−1} characteristic of CS group stretching vibrations, $\nu(\text{CS})$ [9, 23]. In **1** and **2**, these vibrations are shifted to lower frequencies, to 1390 and 700 cm^{−1},

respectively. The shift of CS group stretching vibrations towards lower wavenumbers in **1** and **2** than that in free tu is due to the reduced double bond character between carbon and sulphur atoms [13, 21, 23]. Moreover, for dried sample **2** additional peaks at 1473, 1085, 730 and 630 cm^{-1} can be observed, which are characteristic of $\nu(\text{CN})$ and $\nu(\text{CS})$ in thiourea. According to the IR study, sample **1** is a complex compound where tu is coordinated to the In ion through the sulphur atom. Similar behaviour is reported for the Cd, Cu and Zn chloride complexes with thiourea [9, 13, 14]. Sample **2** is composed of a thiourea complex compound and free thiourea.

According to XRD (XRD patterns not presented), powders **1** and **2** are crystalline materials. XRD patterns of **1** and **2** remained unidentified. Both **1** and **2** contain no InCl_3 as a starting material, replica characteristic of $\text{SC}(\text{NH}_2)_2$ phase (JCPDS Card No. 00-031-1934) [24] were present in the XRD pattern of **2**.

According to the elemental analysis, the composition of **1** (found, in mass%) is: S 20.1%, C 7.7%, N 18.8%, H 2.3%, Cl 23.4% and the composition of **2** (found, in mass%) is: S 27.4%, C 10.3%, N 24.5%, H 3.5%. The composition of **1** is close to that calculated for a compound with a hypothetical formula $\text{InCl}_3 \cdot 3(\text{SCN}_2\text{H}_4)$: In 25.5%, Cl 23.7%, S 21.4%, C 8.0%, N 18.7%, H 2.7%. The composition of **2** is close to that calculated for a mixture of $(\text{InCl}_3 \cdot 3(\text{SCN}_2\text{H}_4)) + 3(\text{SCN}_2\text{H}_4)$: In 17.0%, S 28.4%, C 10.6%, N 24.8%, H 3.5%.

According to the results of the FTIR spectroscopy and chemical analyses, powder **1** is a complex compound

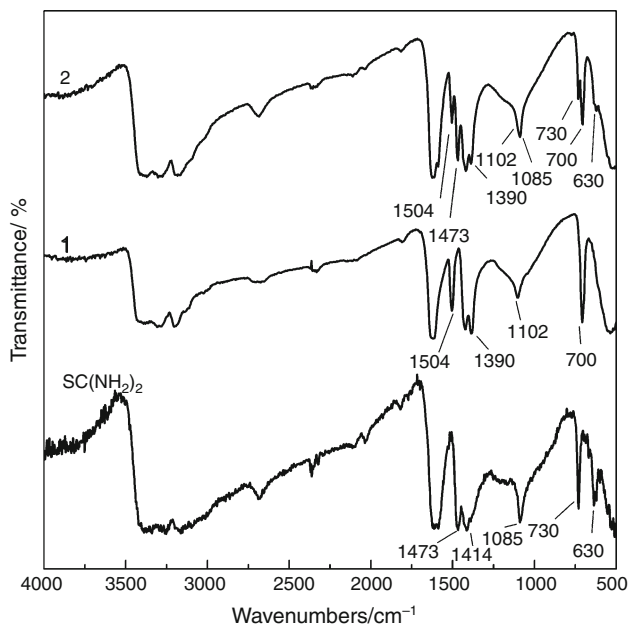


Fig. 1 FTIR spectra of dried samples **1**, **2** and thiourea ($\text{SC}(\text{NH}_2)_2$) recorded at room temperature

where three $\text{SC}(\text{NH}_2)_2$ molecules are coordinated to one In^{3+} cation of the InCl_3 molecule with a general formula $\text{InCl}_3 \cdot 3(\text{SC}(\text{NH}_2)_2)$. A similar compound has been precipitated from aqueous solutions containing InCl_3 and $\text{SC}(\text{NH}_2)_2$ in the molar ratios of 1:1 and 1:3 [25]. Powder **2** is a mixture of **1** and $\text{SC}(\text{NH}_2)_2$.

Thermal analysis

Figures 2a and b show the TG, DTG, DTA curves of samples **1** and **2**, respectively. According to DTG, the thermal degradation of both **1** and **2** in the temperature interval of 30–900 °C in air (80%Ar + 20%O₂) consists of four mass loss steps (Fig. 2a, b; Table 1).

The thermal decomposition of **1** takes place in the interval of 205–730 °C with a total mass loss of 89.1% (Fig. 2a). The first mass loss step occurs in the temperature range of 205–300 °C with a DTG maximum at 230 °C and a mass loss of ca., 34%. The DTA curve shows two sequential endothermic processes with maxima at 210 and 220 °C undergoing a strong exothermic effect with a maximum at 230 °C, and followed by an endothermic effect at 270 °C. The first endothermic effect that peaked at 210 °C obviously corresponds to the melting of **1**. Thermal decomposition of **1** takes place instantly after melting, indicated by the endothermic effect at 220 °C. Exothermic effect with a maximum at 230 °C is obviously due to the sudden oxidation of the evolved CS_2 vapour (see section Study of gaseous and solid products of thermal decomposition). The second decomposition step (300–520 °C) with the DTG maximum at 355 °C and a mass loss of 26.4% is an endothermic process with the DTA maximum at 355 °C. The third decomposition step (520–680 °C) with the DTG maximum at 590 °C involves exothermic reactions with maxima at 580, 610 and 650 °C. The fourth decomposition step in the temperature region of 680–730 °C contains an exothermic process that peaked at 710 °C with the DTG maximum at 715 °C. The characteristic mass losses of the third and fourth decomposition steps are 24.6 and 3.3%, respectively.

The thermal decomposition of **2** takes place in the temperature interval of 180–790 °C in four steps, with a total mass loss of 78.5% (Fig. 2b). Thermal behaviour of **2** is more complex than that of **1**. The endothermic effects detected at 160 and 205 °C obviously belong to the melting and the decomposition of thiourea, respectively [19], as in addition to the complex compound, **2** contains free, non-coordinated thiourea. Endothermic effects at 210 and 220 °C, characteristic of melting and decomposition of the complex compound, are less pronounced than in the case of **1** (Fig. 2b) due to the exothermic processes placed at 215 and 240 °C. The second mass loss step in the temperature interval of 300–400 °C is an endothermic reaction with the

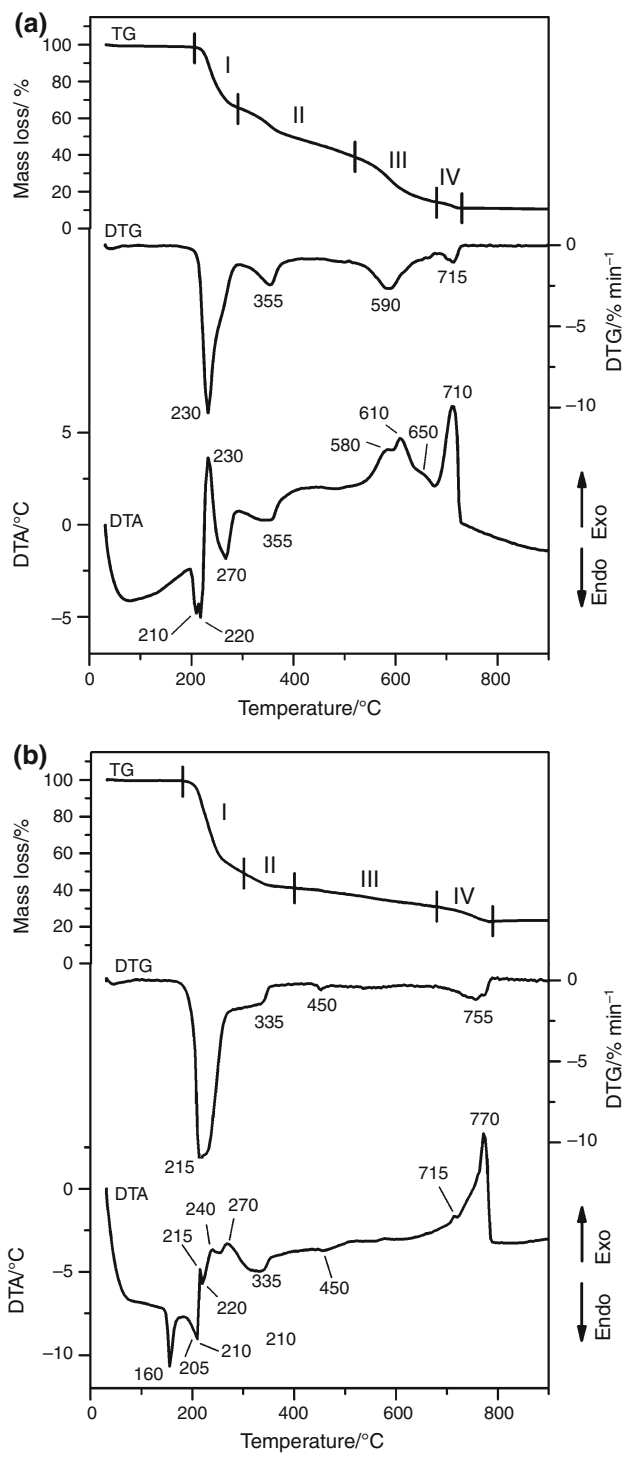


Fig. 2 Simultaneous TG, DTG and DTA curves of **1** (a) and **2** (b). Flowing 80%Ar + 20%O₂: 60 mL min⁻¹, heating rate: 10 °C min⁻¹, initial sample mass for **1** – 7.8 mg and **2** – 7.4 mg

DTG maximum at 335 °C. The third mass loss step between 400–680 °C is an endothermic reaction with the DTG maximum at 450 °C. The mass losses in the second and third decomposition steps are 9.6 and 10.2%, respectively. The last, fourth, decomposition step (680–790 °C)

involves three exothermic processes with maxima at 715 and 770 °C.

According to XRD, the final decomposition product of **1** and **2** at 900 °C in 80%Ar + 20%O₂ is In₂O₃ (PDF 01-073-6440) [24]. For **1**, the yield of 10.9% is much lower than the calculated 30.9%, which refers to the release of some volatile In species (e.g. InCl₃). For **2**, the yield of 21.5% is close to the theoretical value 20.4%, indicating that the excess of thiourea in the precursor hinders the release of volatile indium species from the system.

The first decomposition step for both **1** and **2** consists of the decomposition of thiourea. The thermal degradation of **1** (Fig. 2a) starts at 205 °C, while in the case of **2** the decomposition begins at a lower temperature, at 180 °C, due to free non-coordinated tu present in the sample (Table 1). The decomposition of **2** is more complex, particularly in the first decomposition step, due to several overlapping endo and exo effects. The main difference in the decomposition behaviour of **1** and **2** is observed in the temperature range of 300–680 °C, showing different mass losses of 51 and 19.8%, respectively. The exothermic effects observed for **1** at 580 and 610 °C do not occur in the case of **2**. The last exo effect of **1** at 710 °C is shifted towards higher temperatures for **2**, and is observed at 770 °C. The decompositions of **1** and **2** are completed at 730 and 790 °C, respectively.

Study of gaseous and solid products of thermal decomposition

FTIR spectra of the evolved gases obtained by a TG/DTG analysis coupled with simultaneous EGA-FTIR measurements were used to study gaseous species evolved over the thermal degradation of **1** and **2**. Figure 3 depicts the FTIR spectrum of gases evolved from **1** at 240 °C in 80%Ar + 20%O₂. The evolution profiles of gaseous species from **1** and **2** are compared in Fig. 4.

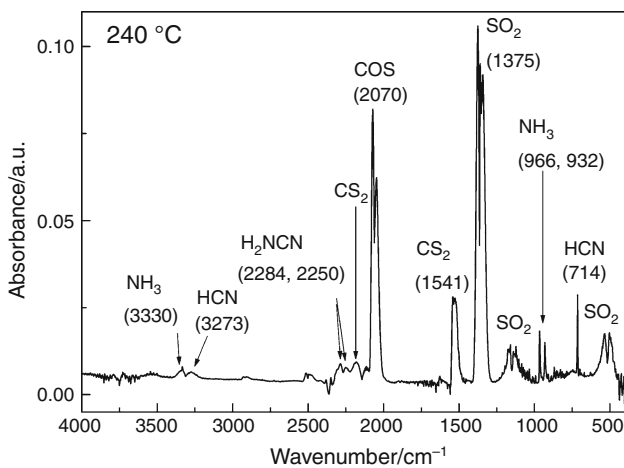
The evolution of carbon disulphide (CS₂) starts at 210 °C from **1** and at 200 °C from **2**, accompanied by the release of ammonia (NH₃) and a small amount of cyanamide (H₂NCO), which are the decomposition products of adjacent thiourea ligands in the melt (Eq. 1) [9, 19].



Evolution of CS₂ from **2** occurs in two steps, as shown in Fig. 4. The first evolution step issues from the decomposition of free thiourea, the second step from the decomposition of the complex compound. Isothiocyanic acid (HNCS) also evolves in the early stage of decomposition, but in a very small amount. Evolution of HNCS could occur according to the reaction (2), as reported previously [9].

Table 1 Decomposition steps, mass losses and temperatures of DTA and DTG peaks of dried powders of **1** and **2**, recorded using the heating rate of 10 °C min⁻¹ in 80%Ar + 20%O₂ atmosphere on the SetSys-Evolution instrument

Sample	Step	TG temp. range/°C	DTG _{max} /°C	DTA peak (±)/°C	Mass loss/%
1	1	205–300	230	210 (–) 220 (–) 230 (+) 270 (–)	34.8
	2	300–520	355	355 (–)	26.4
	3	520–680	590	580 (+) 610 (+) 650 (+)	24.6
	4	680–730	715	710 (+)	3.3
Total mass loss					89.1
2	1	180–300	215	160 (–) 205 (–) 210 (–) 215 (+) 220 (–) 270 (+) 240 (+)	50.7
	2	300–400	335	335 (–)	9.6
	3	400–680	450	450 (–)	10.2
	4	680–790	755	715 (+) 760 (+) 770 (+)	8.0
Total mass loss					78.5

**Fig. 3** EGA-FTIR spectra of evolved gases of **1** at 240 °C. Flowing 80%Ar + 20%O₂; 60 mL min⁻¹, heating rate: 10 °C min⁻¹, initial sample mass: 7.8 mg

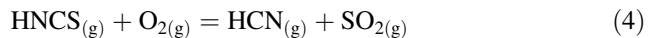
The FTIR spectra of the solid residues (Fig. 5a, b) obtained by heating of **1** up to 225 °C and of **2** up to 180 °C reveal an absorption peak at 2070 cm⁻¹, which can be assigned to the stretching vibration of both thiocyanate

(SCN) and hydrogen bonded RNH₃⁺ groups, and indicate isomerization of thiourea into ammonium thiocyanate [9]. The decomposition of the latter compound could be responsible for gaseous species, such as HNCS and NH₃.

A sudden evolution of carbonyl sulphide (COS) and sulphur dioxide (SO₂) occurs at slightly higher temperatures after the release of CS₂ (Fig. 4). Both COS and SO₂ are the products of the exothermic oxidation of the CS₂ vapour (3) [16, 19]. The maximum evolution of COS and SO₂ takes place close to 240 °C. Hence, the exothermic peaks on the DTA curves of **1** at 230 °C, and of **2** at 215 and 240 °C could be assigned as belonging to the oxidation of the CS₂ vapour.

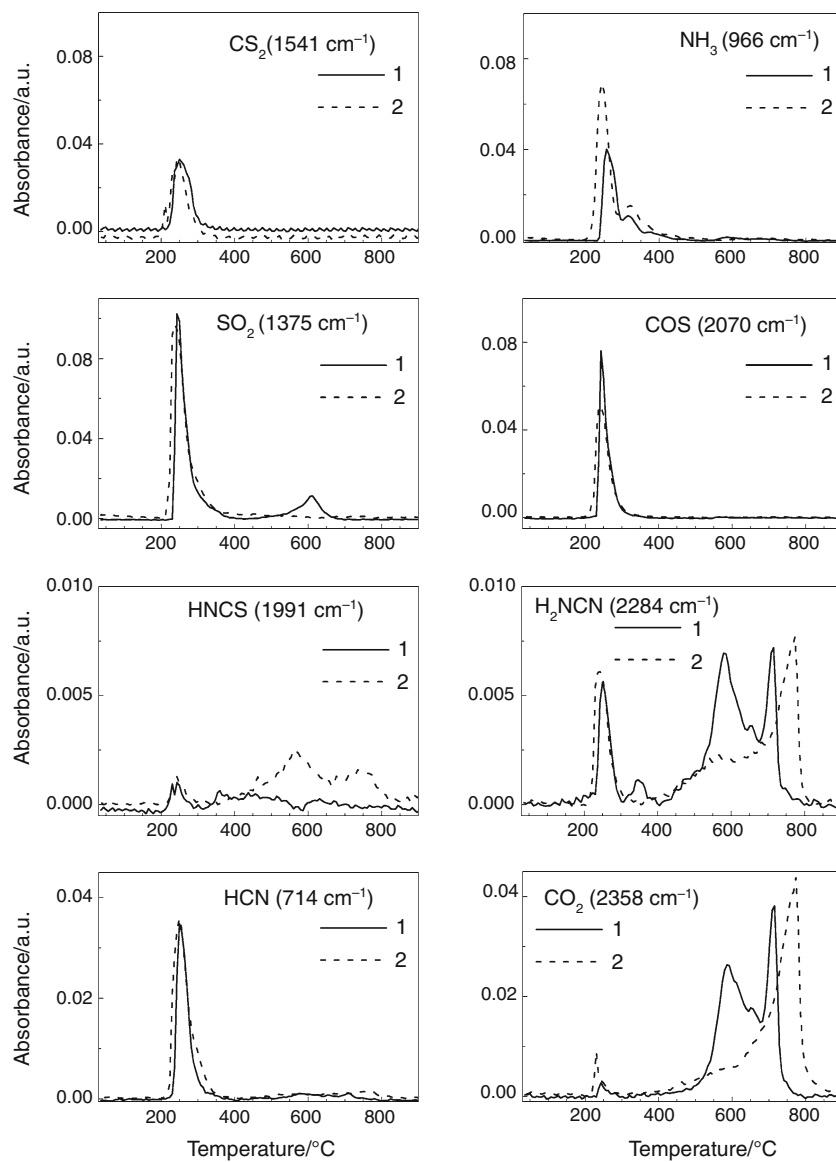


Additionally, the release of hydrogen cyanide (HCN) from **1** and **2** occurs at temperatures higher than 210 °C, reaching the maximum evolution at 250 °C. The release of HCN could be considered as the oxidation product of HNCS according to the reaction (4) [9].



FTIR spectra (Fig. 5a, b) indicate that the solid residues obtained by heating of **1** and **2** up to 300 °C (the end

Fig. 4 Evolution profiles of gases, as determined by TG/EGA-FTIR of **1** (1:3) and **2** (1:6). Flowing 80%Ar + 20%O₂; 60 mL min⁻¹, heating rate: 10 °C min⁻¹, initial sample mass for **1** – 7.8 mg and **2** – 7.4 mg



temperature of the first decomposition step) still contain organic residues. According to XRD the main solid product at 300 °C is In₂S₃, while traces of InCl₃ are present in **1** (Table 2).

In the temperature interval of 300–400 °C, both **1** and **2** show endothermic decomposition reactions and evolution of NH₃, while H₂NCN and HNCS are released only from **1** (Fig. 4). In the case of **2**, evolution of H₂NCN and HNCS takes place at temperatures above 400 °C, with a delay compared to **1**. The re-occurrence of the evolution of H₂NCN could suggest the formation of indium cyanamide.

Indeed, the FTIR spectra of the solid residues of **1** and **2** prepared by heating up to 520 °C (Fig. 5 a, b) show absorptions around 2100 and 695 cm⁻¹ characteristic of the cyanamide group [12, 26]. In addition, the spectrum of **2** shows weak absorptions in the wavenumber range of 1650–1200 cm⁻¹ and at 780 cm⁻¹, which could belong to a

polymerized product of cyanamide [27]. This speculation is supported by the fact that a strong evolution of H₂NCN occurs above 500 °C (Fig. 4).

According to XRD, the solid product of **1** at the end of the second decomposition step (520 °C) contains crystalline phases of In₂S₃, In_{2.24}(NCN)₃ and In₂O₃ (Table 2). Thus, the formation of In_{2.24}(NCN)₃ supposed according to FTIR (Fig. 5a) is confirmed by XRD. The formation of In_{2.24}(NCN)₃ could take place similarly to that observed for ZnCN₂ [12]. In the present case, indium cyanamide is formed probably by the reaction of InCl₃ and H₂NCN, the latter evolving from the decomposition of the complex in the first decomposition step. The solid product of **2** obtained by heating up to 520 °C contains crystalline In₂O₃ and traces of In₂S₃ (Table 2).

In the third decomposition step of **1** (520–680 °C) the exothermic effects at 580 and 650 °C (Fig. 2a) are

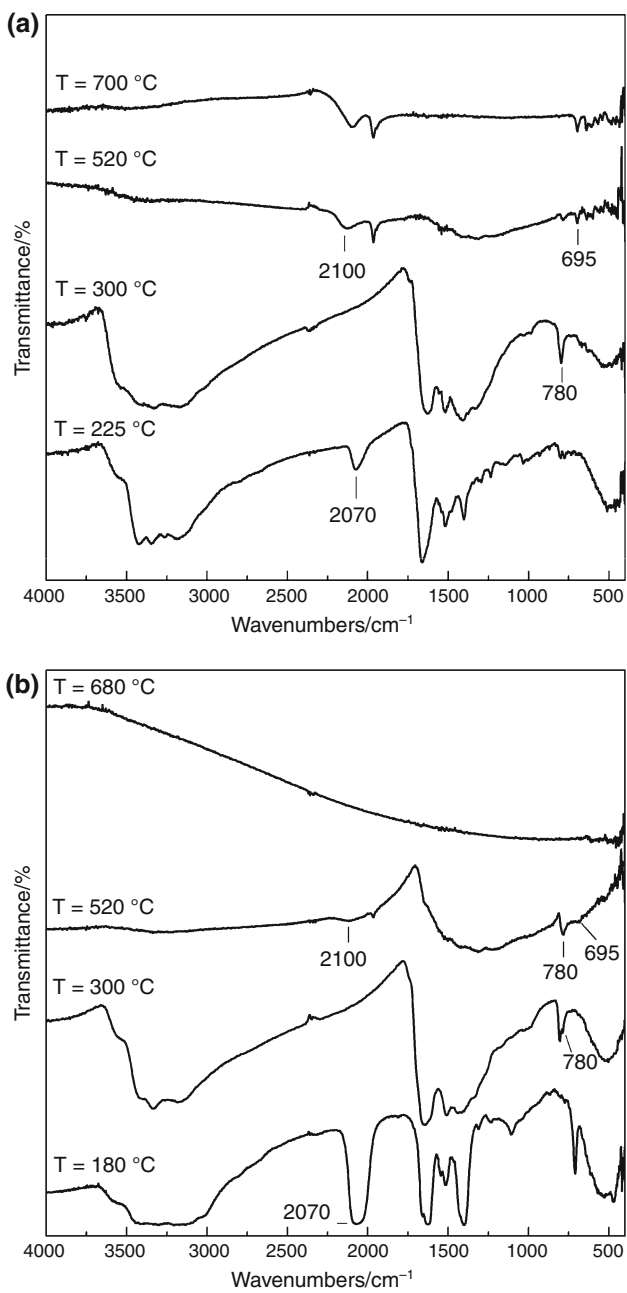
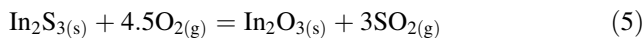


Fig. 5 FTIR spectra of solid residues of **1** (a) and **2** (b) at the end of the decomposition steps

accompanied by an intensive evolution of CO_2 and H_2NCN with strikingly similar evolution profiles (Fig. 4), indicating to the decomposition and combustion of organic pieces. The exothermic effect that peaked at 610 °C (Fig. 2a) is accompanied by the evolution of SO_2 with maxima also at 610 °C (Fig. 4). The evolution of SO_2 is probably due to the oxidation of In_2S_3 according to Eq. (5).



The FTIR spectrum of the solid product of **1** at 700 °C (Fig. 5a) still shows vibrations at the 2100 and 700 cm^{-1}

characteristic of In-cyanamide [26]. This result is in accordance with the XRD study, showing the presence of the crystalline $\text{In}_{2.24}(\text{NCN})_3$ phase in addition to the In_2O_3 and traces of In_2S_3 in the solid product obtained by heating of **1** up to 700 °C in 80%Ar + 20%O₂ (Table 2).

Thermal behaviour of **2** in the temperature interval of 400–680 °C differs significantly from that of **1**. Evolution profiles of H_2NCN and CO_2 show a monotonous increase in this temperature interval without any distinct maxima, while a continuous evolution of HNCS is observed in this temperature range (Fig. 4). The evolution of SO_2 from **2** was observed up to 400 °C, and the evolution of a relatively small amount of SO_2 takes place also in this temperature range, and continues up to 780 °C (Fig. 4).

According to FTIR, the solid residue of **2** at 520 °C indicates relatively weak absorptions at 2100 and 695 cm^{-1} (Fig. 5b) characteristic of $\text{C}\equiv\text{N}$ [26] in In-cyanamide, while absorption bands in the region of 1600–1000 cm^{-1} indicate the presence of organic residues. The solid residue at 680 °C (Fig. 5b) shows no vibrations at 2100 and 690 cm^{-1} characteristic of $\text{C}\equiv\text{N}$ in In-cyanamide. According to XRD, the main solid product of **2** at 520 °C is In_2O_3 with traces of In_2S_3 (Table 2). The solid product at 680 °C consists of the crystalline In_2O_3 phase.

At temperatures above 700 °C, strong exothermic effects occur at 710 and 770 °C for **1** and **2**, respectively (Fig. 2a, b). The evolution of CO_2 and H_2NCN with strikingly similar profiles was recorded for both samples in this final decomposition step (Fig. 4). In addition, the continuous release of HNCS recorded from **2** in the temperature interval of 700–800 °C confirms further decomposition of an organic matter [12].

Probably the decomposition of $\text{In}_{2.4}(\text{NCN})_3$ accompanied by the evolution of H_2NCN and the combustion of organic pieces that leads to the evolution of CO_2 are characteristic reactions for **1** in this step, resulting in In_2O_3 as the final product. The release of H_2NCN from **2** (Fig. 4), where no $\text{In}_{2.4}(\text{NCN})_3$ phase was observed in the solid residue at 680 °C (Table 2), could originate from the decomposition of polymerization products formed at lower temperatures [9]. According to the literature, H_2NCN evolved in the first decomposition step (200–300 °C) is highly reactive and it may react with other decomposition products or polymerize [9]. It could be speculated that the presence of polymerization products affects the decomposition of **2**, shifting the formation of the pure In_2O_3 phase towards higher temperatures. This assumption is supported by the TG data (Table 1) showing that the characteristic mass loss of the final decomposition step (680–730 °C) of **1** (3.3%) is significantly lower than that observed for **2** (8.0%) in the temperature interval of 680–790 °C. This indicates that the content of organic matter in **2** is significantly larger than in **1** at the beginning of the last decomposition step.

Table 2 Crystalline decomposition products of **1** and **2**, as detected by XRD. Heat treatments were performed in a preparative scale in air in laboratory oven

1 (In:S = 1:3)		2 (In:S = 1:6)	
T/°C	Main crystalline phases and JCPDS reference files	T/°C	Main crystalline phases and JCPDS reference files
300	α -In ₂ S ₃ (01-084-1385) (InCl ₃ (00-034-1145))	300	α -In ₂ S ₃ (01-084-1385)
410	β -In ₂ S ₃ (01-074-7284) In ₂ O ₃ (01-073-6440)	410	β -In ₂ S ₃ (01-074-7284)
520	In ₂ O ₃ (01-073-6440) In _{2.24} (NCN) ₃ (00-051-0853) (β -In ₂ S ₃ (01-074-7284))	520	In ₂ O ₃ (01-073-6440) (β -In ₂ S ₃ (01-074-7284))
700	In ₂ O ₃ (01-073-6440) In _{2.24} (NCN) ₃ (00-051-0853)	680	In ₂ O ₃ (01-073-6440)
900	In ₂ O ₃ (01-073-6440)	820	In ₂ O ₃ (01-073-6440)

Conclusions

According to FTIR and XRD, samples **1** and **2** obtained by drying aqueous solutions of InCl₃ and SC(NH₂)₂ at the molar ratios of In:S = 1:3 (**1**) and 1:6 (**2**) contain a complex compound, where SC(NH₂)₂ is coordinated to In atom via S atom. **1** does not contain free SC(NH₂)₂, while in **2** free SC(NH₂)₂ is also present. According to the elemental analyses, the composition of the dried sample **1** is close to a compound with the hypothetical formula InCl₃·3(SCN₂H₄), and **2** is a mixture of phases InCl₃·3(SCN₂H₄) + 3 SCN₂H₄.

The thermal decomposition of **1** in the temperature range of 205–730 °C and that of **2** in the temperature interval of 180–790 °C in 80%Ar + 20%O₂ consists of four mass loss steps with a total mass loss of 89.1 and 78.5%, respectively. Thermal degradation of **2** starts at a lower temperature due to the decomposition of non-coordinated SC(NH₂)₂ present in **2**, followed by the decomposition of the complex compound, as recorded for **1**. In the case of both samples, In₂S₃ is formed in the first decomposition step and In₂O₃ is the final product. In the first decomposition step, CS₂, NH₃ and H₂NCO evolved as the decomposition products of thiourea, which upon oxidation yield to the evolution of COS, SO₂, HCN and CO₂. Thermal degradation of **1** and **2** are similar in the first decomposition step, differences appear at higher temperatures. Above 400 °C, the decomposition steps of **2** are shifted towards higher temperatures than those of **1**. Nevertheless, intensive evolution of H₂NCO and CO₂ with strikingly similar profiles is characteristic of both. It should be noticed that the release of volatile indium species and the formation of In_{2.24}(NCN)₃ as an intermediate decomposition product is hindered in the case of **2**.

This study shows for the first time that the formation of In₂S₃ in the spray pyrolysis process occurs through an indium chloride thiourea complex compound, supposedly of InCl₃·3(SCN₂H₄) formed in an aqueous spray solution containing an appropriate molar ratio of InCl₃ and SC(NH₂)₂. Thermal decomposition of the complex compound is a complicated process, where metal sulphide is formed in the first decomposition step at temperatures below 300 °C, which is similar to that previously reported for cadmium, zinc and copper sulphide formation in the spray process [9, 10, 12].

The thermal decomposition of the precursors for In₂S₃ thin films by the CSP method depends on the In:S molar ratio in the solution. Results of the current study show that an aqueous spray solution with the In:S molar ratio of 1:6 and deposition temperatures up to 400 °C are preferred to deposit In₂S₃ thin films by the spray pyrolysis method in 80%Ar + 20%O₂ to minimize the formation of the In₂O₃ phase. At the same time the deposition of solutions with the In:S molar ratio of 1:6 may result in a high amount of organic residues in the film.

In order to determine the composition and structure of the complex, it should be prepared as a single crystal. To identify the thermal decomposition reactions more precisely, additional studies are needed. Therefore, the TG/DTA studies of the complex should be complemented by the EGA-MS investigations in air and in an inert atmosphere, and then compared to the results of the EGA-FTIR reported in this communication.

Acknowledgements Financing by the Estonian Ministry of Education and Research under project SF0140092s08 and the Estonian Science Foundation under grants ETF6954 and ETF7788 are gratefully acknowledged. The authors thank Mrs. R. Aluvee and Mrs. A. Vaarmann for the elemental analysis. Dr. J. Madarász is thanked for the literature reference. K. Otto acknowledges the graduate school

“Functional materials and processes” for funding from the European Social Fund under the project 1.2.0401.09-0079.

References

- Barreau N. Indium sulfide and relatives in the world of photovoltaics. *Sol Energy*. 2009;83:363–71.
- Hariskos D, Spiering S, Powalla M. Buffer layers in Cu(In, Ga)Se₂ solar cells and modules. *Thin Solid Films*. 2005;480–481: 99–109.
- Lucena R, Aguilera I, Palacios P, Wahnón P, Conesa JC. Synthesis and spectral properties of nanocrystalline V-substituted In_2S_3 , a novel material for more efficient use of solar radiation. *Chem Mater*. 2008;20:5125–7.
- Krunks M, Kärber E, Katerski A, Otto K, Oja Acik I, Dedova T, Mere A. Extremely thin absorber layer solar cells on zinc oxide nanorods by chemical spray. *Sol Energy Mater Sol Cells*. 2010; 94:1191–5.
- Buecheler S, Corica D, Guettler D, Chirila A, Verma R, Müller U, Niesen TP, Palm J, Tiwari AN. Ultrasonically sprayed indium sulfide buffer layers for Cu(In, Ga)(S, Se)₂ thin-film solar cells. *Thin Solid Films*. 2009;517:2312–5.
- Kim WT, Kim CD. Optical energy gaps of β - In_2S_3 thin films grown by spray pyrolysis. *J Appl Phys*. 1986;60:2631–3.
- Otto K, Katerski A, Mere A, Volobujeva O, Krunks M. Spray pyrolysis deposition of indium sulfide thin films. *Thin Solid Films*. 2011;519:3055–60.
- Ratheesh Kumar PM, John TT, Sudha Kartha C, Vijayakumar KP. SHI induced modifications in spray pyrolysed β - In_2S_3 thin films. *Nucl Instrum Methods Phys Res B*. 2006;244:171–3.
- Krunks M, Madarász J, Hiltunen L, Mannonen R, Mellikov E, Niinistö L. Structure and thermal behaviour of dichlorobis(thiourea)cadmium(II), a single-source precursor for CdS thin films. *Acta Chem Scand*. 1997;51:294–301.
- Krunks M, Leskelä T, Mutikainen I, Niinistö L. A thermoanalytical study of copper(I) thiocarbamide compounds. *J Therm Anal Calorim*. 1999;56:479–84.
- Madarász J, Bombicz P, Okuya M, Kaneko S. Thermal decomposition of thiourea complexes of Cu(I), Zn(II), and Sn(II) chlorides as precursors for the spray pyrolysis deposition of sulfide thin films. *Solid State Ion*. 2001;141–142:439–46.
- Krunks M, Madarász J, Leskelä T, Mere A, Niinistö L, Pokol G. Study of zinc thiocarbamide chloride, a single-source precursor for zinc sulfide thin films by spray pyrolysis. *J Therm Anal Calorim*. 2003;72:497–506.
- Bombicz P, Mutikainen I, Krunks M, Leskelä T, Madarász J, Niinistö L. Synthesis, vibrational spectra and X-ray structures of copper(I) thiourea complexes. *Inorg Chim Acta*. 2004;357: 513–25.
- Bombicz P, Madarász J, Krunks M, Niinistö L, Pokol G. Multiple secondary interaction arrangement in the crystal structure of dichlorobis(thiourea-S)-zinc(II). *J Coord Chem*. 2007;60:457–64.
- Dedova T, Krunks M, Volobujeva O, Oja I. ZnS thin films deposited by spray pyrolysis technique. *Phys Stat Sol C*. 2005; 2:1161–6.
- Madarász J, Krunks M, Niinistö L, Pokol G. Evolved gas analysis of dichlorobis(thiourea)zinc(II) by coupled TG-FTIR and TG/DTA-MS techniques. *J Therm Anal Calorim*. 2004;78:679–86.
- Rasika Dias HV. Indium and thallium. In: McCleverty JA, Meyer TJ, editors. *Comprehensive coordination chemistry II*. Elsevier: Pergamon Press; 2003. p. 383–425.
- Beddoes RL, Collison D, Mabbs FE, Temperley J. Structures of Trichlorobis(*N,N,N',N'*-tetramethylurea)indium(III) and Trichlorobis(*N,N,N',N'*-tetramethylthiourea)indium(III). *Acta Crystallogr*. 1991;C47:58–61.
- Madarász J, Pokol G. Comparative evolved gas analysis on thermal degradation of thiourea by coupled TG-FTIR and TG/DTA-MS instruments. *J Therm Anal Calorim*. 2007;88:329–36.
- NIST Chemistry Webbook Standard Reference Database No 69, June 2005 Release. <http://webbook.nist.gov/chemistry>.
- El-Bahy GMS, El-Sayed BA, Shabana AA. Vibrational and electronic studies on some metal thiourea complexes. *Vib Spectrosc*. 2003;31:101–7.
- Rajasekaran R, Ushasree PM, Jayavel R, Ramasamy P. Growth and characterization of zinc thiourea chloride (ZTC): a semiconductive nonlinear optical crystal. *J Cryst Growth*. 2001;229:563–7.
- Krunks M, Mellikov E, Bijakina O. Intermediate compounds in formation of copper sulfides by spray pyrolysis. *Proc Estonian Acad Sci Eng*. 1996;2:98–106.
- International Centre for Diffraction Data (ICDD). Powder Diffraction File (PDF), PDF-2 Release 2007.
- Malyarik MA, Ilyukhin AB, Petrosyants SP, Buslaev YA. Geometric isomerism in indium(III) halide-complexes—synthesis and crystalline-structure of [InCl₃(thio)₃] complexes. *Zh Neorg Khim*. 1992;37:1504–8.
- Baldinozzi G, Malinowska B, Rakib M, Durand G. Crystal structure and characterisation of cadmium cyanamide. *J Mater Chem*. 2002;12:268–72.
- Costa L, Camino G. Thermal behaviour of melamine. *J Therm Anal*. 1988;34:423–9.